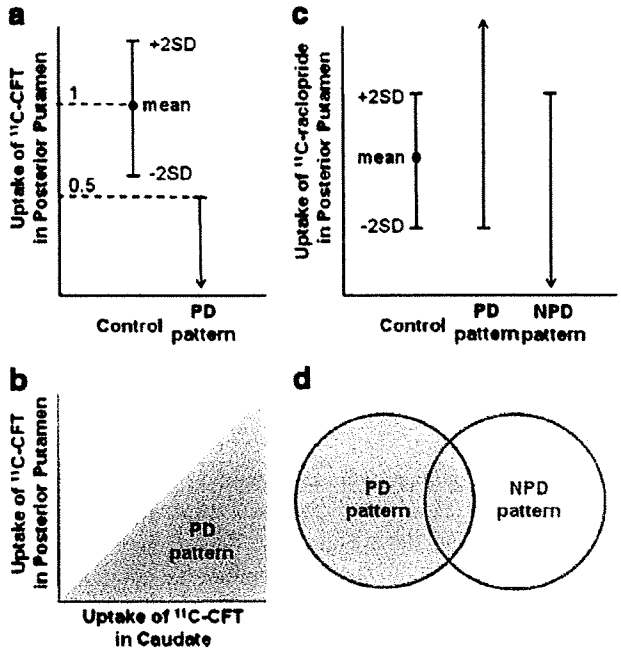

Fig. 2 PD and NPD patterns defined on the basis of dopamine PET findings. PD pattern: ^{11}C-CFT uptake in the posterior putamen of patients less than 50% of the mean uptake in the posterior putamen of normal controls (**a**) and less than that in the caudate of patients (**b**); ^{11}C-raclopride uptake in the posterior putamen of patients more than the mean − 2 SD of the uptake in the posterior putamen of normal controls (**c**). NPD pattern: ^{11}C-raclopride uptake in the posterior putamen of patients less than the mean + 2 SD of the uptake in the posterior putamen of normal controls (**c**). The patient was considered to be PD pattern when both PD and NPD were fulfilled (**d**). The uptake in each subregion of the striatum was evaluated as the average value of both sides

^{11}C-CFT uptake in the posterior putamen of the patients less than 50% of the mean uptake in the posterior putamen of normal controls (Fig. 2a) and less than that in the caudate of the patients (Fig. 2b) and (2) ^{11}C-raclopride uptake in the posterior putamen of the patients more than the mean − 2 SD of the uptake in the posterior putamen of normal controls (Fig. 2c). The NPD pattern was defined as follows: ^{11}C-raclopride uptake in the posterior putamen of the patients less than the mean + 2 SD of the uptake in the posterior putamen of normal controls (Fig. 2c). The patient was considered to be PD pattern when both PD and NPD were fulfilled (Fig. 2d).

Statistical analysis

Differences in the averages and variances were tested by Student's t test and one-way analysis of variance, respectively. Correlations between the two groups of patients were assessed by linear regression analysis with Pearson's correlation test; p values of <0.05 were considered statistically significant.

Results

Patients

Classification into PD and NPD groups All 22 patients who fulfilled the UKPDBB PD criteria at initial diagnosis [10] showed the PD pattern on dopamine PET (Fig. 1). They were classified into the PD group. The other 17 patients were further classified according to dopamine PET findings and respective published clinical criteria. Of the 17 patients, 2 showed the PD pattern on dopamine PET. In fact, the symptom manifested was only resting tremor at initial diagnosis; however, during the course of the study, they fulfilled the UKPDBB PD criteria [10] and were classified into the PD group.

Of the 17 patients, 15 showed the NPD pattern on dopamine PET and were classified into the NPD group (Fig. 1). These patients were then further divided into three subgroups. Six patients fulfilled the multiple system atrophy (MSA) criteria [33]. Two patients fulfilled the progressive supranuclear palsy (PSP) criteria [34]. For the remaining seven patients, no definitive diagnoses could be established despite follow-up for more than 1 year.

Finally, 24 patients (7 men and 17 women, age range: 60–85 years, mean age ± SD = 71.5±6.8 years) and 15 patients (8 men and 7 women, age range: 65–86 years, mean age ± SD: 76.0±5.5 years) were classified into the PD and NPD groups, respectively.

Demographic data Patient characteristics are summarized in Table 1. In the PD group, 11 patients were drug naive, 7 were being treated with L-dopa and 6 were being treated with L-dopa and dopamine agonists at the time of dopamine PET. The interval between cardiac ^{123}I-MIBG scintigraphy and dopamine PET was within 6 months for 16 patients, between 6 and 12 months for 1 patient and more than 1 year for 7 patients. However, the HY stage of each patient in the PD group remained the same between cardiac ^{123}I-MIBG scintigraphy and dopamine PET. In the NPD group, 11 patients were not administered any antiparkinsonian drug, and 4 were being treated with only L-dopa. The interval between the two examinations was within 6 months for 12 patients, between 6 and 12 months for 1 patient and more than 1 year for 2 patients.

Uptake of ^{123}I-MIBG

Both the early and delayed images showed significantly lower H/M ratios in the PD group than in the NPD group (Fig. 3). In both the early and delayed images, the H/M ratios tended to decrease with the progression of the HY stages; however, the decrease was not statistically significant.

Table 1 Clinical features of patients in Parkinson's disease and non-Parkinson's disease groups

Groups	Patients		Age (years)	Duration (years)	^{123}I-MIBG scintigraphy		^{11}C-CFT PET
	Number	M:F			Heart to mediastinum ratio		Uptake ratio index in the whole striatum
					Early	Delayed	
Parkinson's disease	24	7:17	71.5±6.8	3.5±3.2	1.66±0.45	1.46±0.41	0.98±0.34
Hoehn and Yahr 1	4	0:4	65.0±7.7	2.9±2.6	1.75±0.33	1.49±0.29	1.49±0.40
Hoehn and Yahr 2	9	2:7	73.9±5.6	2.4±1.0	1.81±0.54	1.60±0.45	1.00±0.20
Hoehn and Yahr 3	8	5:3	71.9±7.2	3.0±1.8	1.57±0.44	1.41±0.44	0.81±0.20
Hoehn and Yahr 4	3	0:3	72.3±5.0	9.0±6.1	1.36±0.05	1.12±0.08	0.69±0.07
Non-Parkinson's disease	15	8:7	76.0±5.5	2.8±1.9	2.35±0.46	2.18±0.51	1.65±0.68

Data are expressed as mean±SD

Table 2 shows the sensitivity and specificity of cardiac ^{123}I-MIBG scintigraphy in differentiating patients with PD from the other patients with chief complaints of parkinsonian symptoms. When the optimal cut-off levels of ^{123}I-MIBG were set at 1.95 and 1.60 by receiver-operating characteristic analysis, the sensitivity of cardiac ^{123}I-MIBG scintigraphy for the diagnosis of PD was 79.2 and 70.8% and the specificity was 93.3 and 93.3% in the early image and delayed images, respectively. In HY 1 and 2 PD patients the sensitivity was 69.2 and 53.9% and in HY 3 and 4 PD patients the sensitivity was 90.9 and 90.9% in the early image and delayed images, respectively

Uptake of ^{11}C-CFT

The uptake of ^{11}C-CFT in the whole striatum decreased with the progression of the HY stages (Fig. 4). Significant reduction in the ^{11}C-CFT uptake with the progression of the HY stages was also observed in each of the three subregions of the striatum. Correlation between cardiac ^{123}I-MIBG scintigraphy and ^{11}C-CFT PET was evaluated in the 16 patients who underwent the two examinations within 6 months. There was no significant correlation between the ^{11}C-CFT uptake in the whole striatum and the H/M ratios in both the early images (r=0.15, p=0.59) and delayed images (r=0.21, p=0.43) (Fig. 5). Further, no significant correlation was observed between the ^{11}C-CFT uptake in each of the three subregions of the striatum and the H/M ratio.

Discussion

In the present study, we investigated the sensitivity and specificity of cardiac ^{123}I-MIBG scintigraphy in diagnosing PD and differentiating the patients with PD from the others with chief complaints of parkinsonian symptoms. Further, we investigated the correlation between cardiac sympathetic function assessed by cardiac ^{123}I-MIBG uptake, nigrostriatal

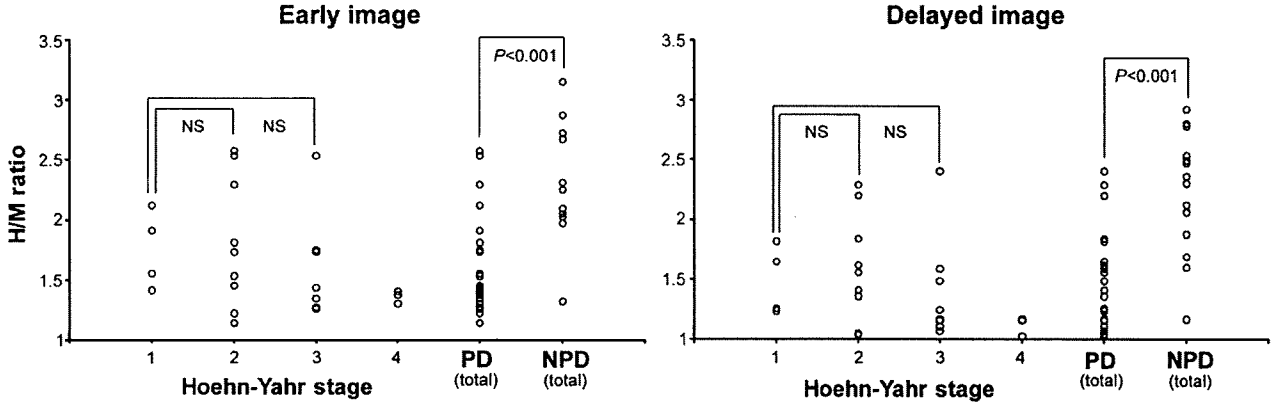

Fig. 3 H/M ratios in the PD and NPD groups in early and delayed images. Each graph represents the relation between the H/M ratio and Hoehn and Yahr stage of PD and a comparison of the H/M ratios of the total number of PD and NPD patients. Both images showed that the H/M ratios were significantly lower in the PD group than in the NPD group; however, the H/M ratios of patients in HY 1 of PD were not significantly higher than those of the patients in HY 2 and 3 of PD. *NS* not significant

Table 2 Sensitivity and specificity of cardiac ^{123}I-MIBG scintigraphy in differentiating Parkinson's disease from other parkinsonian syndromes

Total PD patients (n=24)												
	Early image						Delayed image					
Cut-off	1.80	1.85	1.90	1.95	2.00	2.05	1.60	1.65	1.70	1.75	1.80	1.85
Sensitivity	70.8%	75.0%	75.0%	79.2%	79.2%	79.2%	70.8%	75.0%	79.2%	79.2%	79.2%	87.5%
Specificity	93.3%	93.3%	93.3%	93.3%	86.7%	80.0%	93.3%	80.0%	73.3%	73.3%	73.3%	73.3%
Hoehn and Yahr 1 and 2 (n=15)												
	Early image						Delayed image					
Cut-off	1.80	1.85	1.90	1.95	2.00	2.05	1.60	1.65	1.70	1.75	1.80	1.85
Sensitivity	53.8%	61.5%	61.5%	69.2%	69.2%	69.2%	53.8%	61.5%	69.2%	69.2%	69.2%	84.6%

Cut-off levels, for which both the sensitivity and specificity were more than 70%, are shown. The optimal cut-off levels determined by receiver-operating characteristic analysis were at 1.95 and 1.60 in the early and delayed images, respectively

dopaminergic function assessed by ^{11}C-CFT uptake and disease stage determined according to the HY scale.

It has been reported that cardiac ^{123}I-MIBG uptake in patients with PD is significantly lower than that in patients with other parkinsonian syndromes [1–7]; this result corresponds to our results. Several reports suggest that the severity of motor impairment and disease duration are correlated with reduced ^{123}I-MIBG uptake in patients with PD [1, 2, 5, 6]; however, some other findings deny such correlations, similar to ours [3, 4, 7, 8]. This discrepancy is presumably explained by the fact that the degree of cardiac ^{123}I-MIBG uptake in patients in HY 1 and 2 of PD varies greatly among different studies. Difficult definitive diagnosis of PD in early and mild cases may also be because of the great variation. On the other hand, almost all patients in the advanced stage of PD have shown very low ^{123}I-MIBG uptake in both the previous and the present studies. Li et al. reported that cardiac sympathetic denervation progresses over time and that the rate of decrease in the number of sympathetic terminals appears to be at least as high as that of nigrostriatal dopaminergic terminals [35]. Therefore, we considered that although the onset of cardiac sympathetic denervation varied among the patients with PD, severe cardiac sympathetic denervation occurred in all of the patients by the terminal stage of PD. In regard to the association with a sympathetic symptom, it was reported that reduced ^{123}I-MIBG uptake does not always mean the existence of a sympathetic symptom [1, 3, 4, 7]. Also in this study, of the three patients in stage 4 of the HY scale who showed very low ^{123}I-MIBG uptake (Fig. 3), two had orthostatic hypotension; however, the remaining one patient had no cardiovascular sympathetic symptom and showed no abnormality in the head-up tilt test. In contrast to ^{123}I-MIBG uptake, the decrease in ^{11}C-CFT uptake in the whole striatum and in each of its three subregions significantly correlated with disease progression represented by the HY stages, as reported previously [14, 16, 22]. Considering the causal pathophysiological mechanism of PD, this is reasonable because ^{11}C-CFT uptake directly indicates nigrostriatal dopaminergic function.

We investigated the sensitivity and specificity of cardiac ^{123}I-MIBG scintigraphy in diagnosing PD and differentiating the patients with PD from the other patients with chief complaints of parkinsonian symptoms. Similar to the

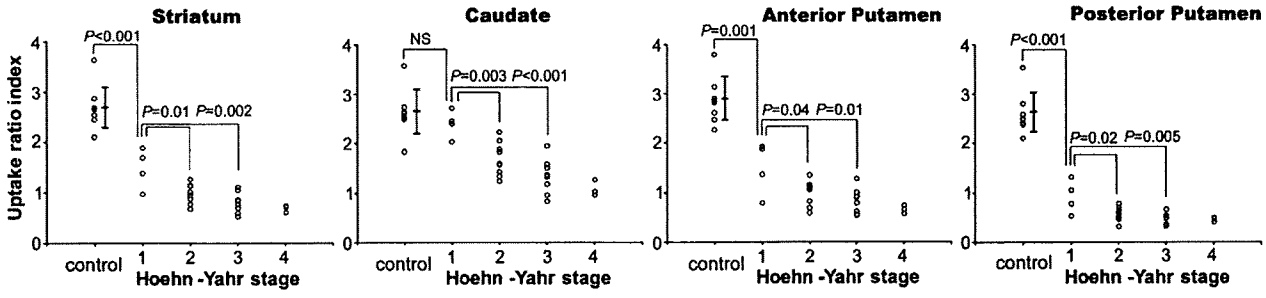

Fig. 4 Relation between the HY stage and uptake ratio index of ^{11}C-CFT in the whole striatum, caudate, anterior putamen and posterior putamen of patients with PD. In all four graphs, the uptakes in the patients in HY 1 of PD are significantly higher than those in the patients in HY 2 and 3 of PD. The uptakes in the caudate of patients in HY 1 of PD are not significantly higher than those in the caudate of controls, while the uptakes in the whole striatum, anterior putamen and posterior putamen of patients in HY 1 of PD are significantly higher than those in the corresponding regions of the controls. The *vertical bar* represents the mean ± SD of controls. *NS* not significant

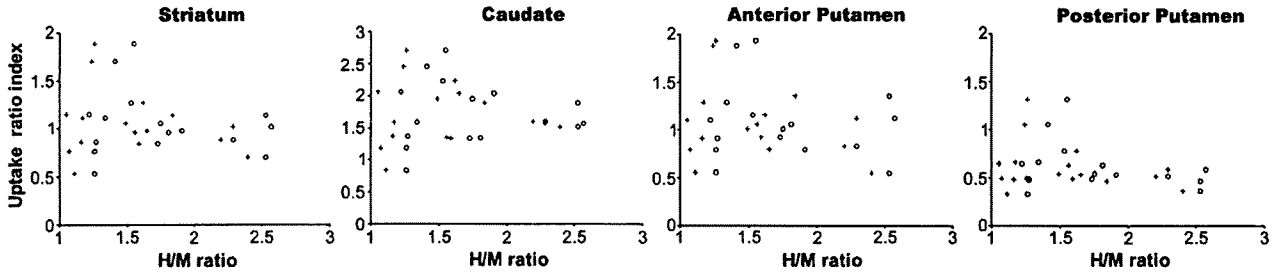

Fig. 5 Relation between the H/M ratio and uptake ratio index of ^{11}C-CFT in the whole striatum, caudate, anterior putamen and posterior putamen of patients with PD. Correlation was evaluated for 16 patients who underwent the two examinations (scintigraphy and PET) within 6 months. In all four graphs, no significant correlations are observed between the early images (*open circles*) and delayed images (*plus signs*)

previous meta-analysis of studies with a total of 246 PD cases [36], in both early and delayed images our study showed high specificity for the overall cases and high sensitivity for the advanced cases. However, early cases tended to have relatively lower sensitivity in both images, although the sample size and methodology greatly differed among the studies. Thus, our results suggested that even in the case of sustained cardiac ^{123}I-MIBG uptake, the possibility of PD should not be denied and follow-up clinical examinations, including ^{123}I-MIBG scintigraphy, should be conducted, especially in early and mild PD cases.

No definite correlation was found either between cardiac ^{123}I-MIBG uptake and striatal ^{11}C-CFT uptake or between cardiac ^{123}I-MIBG uptake and subregional ^{11}C-CFT uptake in the PD group. Two groups have reported the association between the functional impairment of the nigrostriatal dopaminergic system and that of the cardiac sympathetic system [8, 37]. Spiegel et al. (n=18) found a correlation between the two indices, i.e. ^{123}I-MIBG and ^{11}C-CFT uptake, while Raffel et al. (n=9) found no correlation between them. This discrepancy may be explained as follows. The functional impairment of both the nigrostriatal dopaminergic and cardiac sympathetic systems increases with disease progression, as described earlier; hence, a correlation was observed in some studies. On the other hand, there is no report that suggests a direct cause-effect relationship between the functional impairment of the nigrostriatal dopaminergic system and that of the cardiac sympathetic system. Thus, a statistically significant correlation between the functional impairments of the two systems may depend on the sample size and methodology. However, the functional impairments of the two systems would, in fact, occur and progress independently. Sometimes, impairment of the cardiac sympathetic function may precede that of the nigrostriatal dopaminergic function, while at other times, the latter may precede the former.

This is the first report wherein PD and NPD patterns in dopamine PET findings were defined on the basis of the results which have been confirmed as follows. In presynaptic DAT images, three characteristic changes are observed [14–16, 22]. First, the reduction in the ^{11}C-CFT uptake in the striatum begins from the posterior putamen, representing the initial locus of PD [38]. Second, the uptake ratio of the posterior putamen to the caudate is less than 1. Third, one putamen is usually more affected than the other, reflecting asymmetric degeneration. In fact, Fig. 4 shows that the ^{11}C-CFT uptake in the posterior putamen markedly decreased in the early stage of PD, while that in the caudate was relatively constant in the early stage. In postsynaptic D_2R images, putaminal uptake is normal or mildly upregulated in untreated PD, presumably as a compensatory response to decrease in presynaptic dopamine [17–19]. On the other hand, in treated or longstanding PD, the uptake restores to the normal level in the putamen and most often decreases in the caudate; this is presumably as a result of long-term downregulation due to chronic dopaminergic therapy or structural adaptation of the postsynaptic dopaminergic system to the progressive degeneration of nigrostriatal neurons [17, 19, 21]. In fact, in vitro studies have reported that the densities of striatal D_2Rs are maintained even in the advanced stage [39, 40].

On the basis of the earlier mentioned characteristic changes, especially in the posterior putamen, we defined the PD and NPD patterns such that false-negative cases should be as few as possible, because the aim was to reinforce the published clinical criteria. For defining the PD pattern, we considered that ^{11}C-CFT uptake in the posterior putamen of the patients should be less than that in the caudate of the patients and less than 50% of the mean uptake in normal controls. This percentage (i.e. 50%) was selected (1) on the basis of previous PET reports and considered suitable to distinguish normal from affected individuals [14–16, 22] and (2) on the basis of previous reports of in vitro studies, stating that parkinsonian symptoms appear when 80% of the striatal dopamine is lost or 50% of the nigral cells degenerate [38, 41]. Asymmetric uptake was not defined because of the difficulty in determining the intraindividual differences in

the uptake on the left and right sides. However, all 24 patients with PD showed asymmetric uptake. In the ^{11}C-raclopride PET image, since the uptake in the putamen was not less than the normal range, we considered that the uptake in the posterior putamen was normal or increased. For defining the NPD pattern, presynaptic function was not determined because the degree of the presynaptic dysfunction varies with diseases. In the ^{11}C-raclopride PET image, we considered that the uptake in the posterior putamen was normal or decreased because the uptake was not more than the normal range, except for Lewy body disease.

Conclusions

In early and mild PD cases, cardiac ^{123}I-MIBG scintigraphy is of limited value in the diagnosis of PD, because the sensitivity was indicated to be less than 70%. However, because of its high specificity for the overall cases and high sensitivity for the advanced cases, cardiac ^{123}I-MIBG scintigraphy may assist in the diagnosis of PD in a complementary role with the dopaminergic neuroimaging. Disease progression indicated by the HY stages has a stronger association with the nigrostriatal dopaminergic function assessed by striatal ^{11}C-CFT uptake than with the cardiac sympathetic function assessed by cardiac ^{123}I-MIBG uptake. The impairment of the two functions would occur and progress independently.

Acknowledgments The authors thank Mr. Keiichi Kawasaki, Dr. Masaya Hashimoto, and Ms. Hiroko Tsukinari for their technical assistance and useful discussions. This work was supported by grant-in-aid for Scientific Research (B) No. 20390334 (Ki.I.) from the Japan Society for the Promotion of Science and a grant (06-46) (Ki.I.) from the Program for Promotion of Fundamental Studies in Health Sciences of the National Institute of Biomedical Innovation of Japan, and a grant-in-aid for Neurological and Psychiatric Research (S.M., Y.S., and Ke.I.), and Research fo Longevity (S.M., Y.S., and Ke.I.) from the Ministry of Health, Labor, and Welfare of Japan, a grant-in-aid for Long-Term Comprehensive Research on Age-associated Dementia from the Tokyo Metropolitan Institute of Gerontology (K.K., S.M., and Ke.I.).

References

1. Orimo S, Ozawa E, Nakade S, Sugimoto T, Mizusawa H. (123)I-metaiodobenzylguanidine myocardial scintigraphy in Parkinson's disease. J Neurol Neurosurg Psychiatry 1999;67:189–94.
2. Satoh A, Serita T, Seto M, Tomita I, Satoh H, Iwanaga K, et al. Loss of 123I-MIBG uptake by the heart in Parkinson's disease: assessment of cardiac sympathetic denervation and diagnostic value. J Nucl Med 1999;40:371–5.
3. Taki J, Nakajima K, Hwang EH, Matsunari I, Komai K, Yoshita M, et al. Peripheral sympathetic dysfunction in patients with Parkinson's disease without autonomic failure is heart selective and disease specific. taki@med.kanazawa-u.ac.jp. Eur J Nucl Med 2000;27:566–73.
4. Takatsu H, Nishida H, Matsuo H, Watanabe S, Nagashima K, Wada H, et al. Cardiac sympathetic denervation from the early stage of Parkinson's disease: clinical and experimental studies with radiolabeled MIBG. J Nucl Med 2000;41:71–7.
5. Nagayama H, Hamamoto M, Ueda M, Nagashima J, Katayama Y. Reliability of MIBG myocardial scintigraphy in the diagnosis of Parkinson's disease. J Neurol Neurosurg Psychiatry 2005;76:249–51.
6. Hamada K, Hirayama M, Watanabe H, Kobayashi R, Ito H, Ieda T, et al. Onset age and severity of motor impairment are associated with reduction of myocardial 123I-MIBG uptake in Parkinson's disease. J Neurol Neurosurg Psychiatry 2003;74:423–6.
7. Braune S, Reinhardt M, Schnitzer R, Riedel A, Lucking CH. Cardiac uptake of [123I]MIBG separates Parkinson's disease from multiple system atrophy. Neurology 1999;53:1020–5.
8. Raffel DM, Koeppe RA, Little R, Wang CN, Liu S, Junck L, et al. PET measurement of cardiac and nigrostriatal denervation in Parkinsonian syndromes. J Nucl Med 2006;47:1769–77.
9. Rajput AH, Rozdilsky B, Rajput A. Accuracy of clinical diagnosis in parkinsonism–a prospective study. Can J Neurol Sci 1991;18:275–8.
10. Hughes AJ, Daniel SE, Kilford L, Lees AJ. Accuracy of clinical diagnosis of idiopathic Parkinson's disease: a clinico-pathological study of 100 cases. J Neurol Neurosurg Psychiatry 1992;55:181–4.
11. Jankovic J, Rajput AH, McDermott MP, Perl DP. The evolution of diagnosis in early Parkinson disease. Parkinson Study Group. Arch Neurol 2000;57:369–72.
12. Hughes AJ, Daniel SE, Lees AJ. Improved accuracy of clinical diagnosis of Lewy body Parkinson's disease. Neurology 2001;57:1497–9.
13. Plotkin M, Amthauer H, Klaffke S, Kuhn A, Ludemann L, Arnold G, et al. Combined 123I-FP-CIT and 123I-IBZM SPECT for the diagnosis of parkinsonian syndromes: study on 72 patients. J Neural Transm 2005;112:677–92.
14. Nurmi E, Bergman J, Eskola O, Solin O, Vahlberg T, Sonninen P, et al. Progression of dopaminergic hypofunction in striatal subregions in Parkinson's disease using [18F]CFT PET. Synapse 2003;48:109–15.
15. Frost JJ, Rosier AJ, Reich SG, Smith JS, Ehlers MD, Snyder SH, et al. Positron emission tomographic imaging of the dopamine transporter with 11C-WIN 35,428 reveals marked declines in mild Parkinson's disease. Ann Neurol 1993;34:423–31.
16. Rinne JO, Ruottinen H, Bergman J, Haaparanta M, Sonninen P, Solin O. Usefulness of a dopamine transporter PET ligand [(18)F] beta-CFT in assessing disability in Parkinson's disease. J Neurol Neurosurg Psychiatry 1999;67:737–41.
17. Antonini A, Schwarz J, Oertel WH, Beer HF, Madeja UD, Leenders KL. [11C]raclopride and positron emission tomography in previously untreated patients with Parkinson's disease: influence of L-dopa and lisuride therapy on striatal dopamine D2-receptors. Neurology 1994;44:1325–9.
18. Kaasinen V, Ruottinen HM, Någren K, Lehikoinen P, Oikonen V, Rinne JO. Upregulation of putaminal dopamine D2 receptors in early Parkinson's disease: a comparative PET study with [11C] raclopride and [11C]N-methylspiperone. J Nucl Med 2000;41:65–70.
19. Rinne JO, Laihinen A, Rinne UK, Någren K, Bergman J, Ruotsalainen U. PET study on striatal dopamine D2 receptor changes during the progression of early Parkinson's disease. Mov Disord 1993;8:134–8.
20. Dentresangle C, Veyre L, Le Bars D, Pierre C, Lavenne F, Pollak P, et al. Striatal D2 dopamine receptor status in Parkinson's disease: an [18F]dopa and [11C]raclopride PET study. Mov Disord 1999;14:1025–30.
21. Antonini A, Schwarz J, Oertel WH, Pogarell O, Leenders KL. Long-term changes of striatal dopamine D2 receptors in patients

with Parkinson's disease: a study with positron emission tomography and [11C]raclopride. Mov Disord 1997;12:33–8.
22. Wang J, Zuo CT, Jiang YP, Guan YH, Chen ZP, Xiang JD, et al. 18F-FP-CIT PET imaging and SPM analysis of dopamine transporters in Parkinson's disease in various Hoehn & Yahr stages. J Neurol 2007;254:185–90.
23. Knudsen GM, Karlsborg M, Thomsen G, Krabbe K, Regeur L, Nygaard T, et al. Imaging of dopamine transporters and D2 receptors in patients with Parkinson's disease and multiple system atrophy. Eur J Nucl Med Mol Imaging 2004;31:1631–8.
24. Kim YJ, Ichise M, Ballinger JR, Vines D, Erami SS, Tatschida T, et al. Combination of dopamine transporter and D2 receptor SPECT in the diagnostic evaluation of PD, MSA, and PSP. Mov Disord 2002;17:303–12.
25. Verstappen CC, Bloem BR, Haaxma CA, Oyen WJ, Horstink MW. Diagnostic value of asymmetric striatal D2 receptor upregulation in Parkinson's disease: an [123I]IBZM and [123I]FP-CIT SPECT study. Eur J Nucl Med Mol Imaging 2007;34:502–7.
26. Fujiwara T, Watanuki S, Yamamoto S, Miyake M, Seo S, Itoh M, et al. Performance evaluation of a large axial field-of-view PET scanner: SET-2400W. Ann Nucl Med 1997;11:307–13.
27. Hashimoto M, Kawasaki K, Suzuki M, Mitani K, Murayama S, Mishina M, et al. Presynaptic and postsynaptic nigrostriatal dopaminergic functions in multiple system atrophy. Neuroreport 2008;19:145–50.
28. Ishibashi K, Ishii K, Oda K, Kawasaki K, Mizusawa H, Ishiwata K. Regional analysis of age-related decline in dopamine transporters and dopamine D2-like receptors in human striatum. Synapse 2009;63:282–90.
29. NK LO, Dolle F, Lundkvist C, Sandell J, Swahn CG, Vaufrey F, et al. Precursor synthesis and radiolabelling of the dopamine D2 receptor ligand [11C]raclopride from [11C]methyl triflate. J Labelled Compd Radiopharm 1999;42:1183–93.
30. Kawamura K, Oda K, Ishiwata K. Age-related changes of the [11C]CFT binding to the striatal dopamine transporters in the Fischer 344 rats: a PET study. Ann Nucl Med 2003;17:249–53.
31. Antonini A, Leenders KL, Reist H, Thomann R, Beer HF, Locher J. Effect of age on D2 dopamine receptors in normal human brain measured by positron emission tomography and 11C-raclopride. Arch Neurol 1993;50:474–80.
32. Nakajima K, Taki J, Tonami N, Hisada K. Decreased 123I-MIBG uptake and increased clearance in various cardiac diseases. Nucl Med Commun 1994;15:317–23.
33. Gilman S, Low PA, Quinn N, Albanese A, Ben-Shlomo Y, Fowler CJ, et al. Consensus statement on the diagnosis of multiple system atrophy. J Auton Nerv Syst 1998;74:189–92.
34. Litvan I, Agid Y, Calne D, Campbell G, Dubois B, Duvoisin RC, et al. Clinical research criteria for the diagnosis of progressive supranuclear palsy (Steele-Richardson-Olszewski syndrome): report of the NINDS-SPSP international workshop. Neurology 1996;47:1–9.
35. Li ST, Dendi R, Holmes C, Goldstein DS. Progressive loss of cardiac sympathetic innervation in Parkinson's disease. Ann Neurol 2002;52:220–3.
36. Braune S. The role of cardiac metaiodobenzylguanidine uptake in the differential diagnosis of parkinsonian syndromes. Clin Auton Res 2001;11:351–5.
37. Spiegel J, Mollers MO, Jost WH, Fuss G, Samnick S, Dillmann U, et al. FP-CIT and MIBG scintigraphy in early Parkinson's disease. Mov Disord 2005;20:552–61.
38. Fearnley JM, Lees AJ. Ageing and Parkinson's disease: substantia nigra regional selectivity. Brain 1991;114(Pt 5):2283–301.
39. Guttman M, Seeman P, Reynolds GP, Riederer P, Jellinger K, Tourtellotte WW. Dopamine D2 receptor density remains constant in treated Parkinson's disease. Ann Neurol 1986;19:487–92.
40. Bokobza B, Ruberg M, Scatton B, Javoy-Agid F, Agid Y. [3H] spiperone binding, dopamine and HVA concentrations in Parkinson's disease and supranuclear palsy. Eur J Pharmacol 1984;99:167–75.
41. Kish SJ, Shannak K, Hornykiewicz O. Uneven pattern of dopamine loss in the striatum of patients with idiopathic Parkinson's disease. Pathophysiologic and clinical implications. N Engl J Med 1988;318:876–80.

Acta Neurol Scand 2010: 121: 127–130 DOI: 10.1111/j.1600-0404.2009.01272.x

ACTA NEUROLOGICA
SCANDINAVICA

Clinical Commentary

Less protease-resistant PrP in a patient with sporadic CJD treated with intraventricular pentosan polysulphate

Terada T, Tsuboi Y, Obi T, Doh-ura K, Murayama S, Kitamoto T, Yamada T, Mizoguchi K. Less protease-resistant PrP in a patient with sporadic CJD treated with intraventricular pentosan polysulphate. Acta Neurol Scand: 2010: 121: 127–130.

Treatment with intraventricular pentosan polysulphate (PPS) might be beneficial in patients with Creutzfeldt–Jakob disease. We report a 68-year-old woman with sporadic Creutzfeldt–Jakob disease who received continuous intraventricular PPS infusion (1–120 μg/kg/day) for 17 months starting 10 months after the onset of clinical symptoms. Treatment with PPS was well tolerated but was associated with a minor, transient intraventricular hemorrhage and a non-progressive collection of subdural fluid. The patient's overall survival time was well above the mean time expected for the illness but still within the normal range. Post-mortem examination revealed that the level of abnormal protease-resistant prion protein in the brain was markedly decreased compared with levels in brains without PPS treatment. These findings suggest that intraventricular PPS infusion might modify the accumulation of abnormal prion proteins in the brains of patients with sporadic Creutzfeldt–Jakob disease.

T. Terada[1], Y. Tsuboi[2], T. Obi[1], K. Doh-ura[3], S. Murayama[4], T. Kitamoto[5], T. Yamada[2], K. Mizoguchi[1]

[1]Department of Neurology, Shizuoka Institute of Epilepsy and Neurological Disorders, Shizuoka, Japan; [2]Department of Neurology, Fukuoka University School of Medicine, Fukuoka, Japan; [3]Division of Prion Biology, Department of Prion Research, Tohoku University Graduate School of Medicine, Sendai, Japan; [4]Department of Neuropathology, Tokyo Metropolitan Institute of Gerontology, Tokyo, Japan; [5]Department of Neurological Science, Tohoku University Graduate School of Medicine, Sendai, Japan

Key words: Creutzfeldt–Jakob disease; intraventricular infusion; pentosan polysulphate; prion protein

Tomokazu Obi, Department of Neurology, Shizuoka Institute of Epilepsy and Neurological Disorders, Urushiyama 886, Aoi-ku, Shizuoka 420-8688, Japan
Tel.: +81 54 245 5446
Fax: +81 54 247 9781
e-mail: obit@szec.hosp.go.jp

Accepted for publication September 3, 2009

Introduction

Current options for the treatment of Creutzfeldt–Jakob disease (CJD) do not slow or halt disease progression. Treatment with pentosan polysulphate (PPS), a large polyglycoside molecule with anti-thrombotic and anti-inflammatory properties, administered intraventricularly to bypass the blood brain barrier can both prolong the survival period and reduce the extent of abnormal prion protein (PrP) deposition in the brains of rodent prion disease models (1). The safety and efficacy of intraventricular PPS treatment in humans with CJD, however, remains largely unknown (2–6). We report a patient with sporadic CJD (sCJD) treated with continuous intraventricular PPS administration starting 10 months after the onset of clinical symptoms.

Case report

The patient was a 68-year-old woman with neither a family history of prion disease nor previous history of neurological disease. She had never received cadaveric growth hormone injection, a dura mater transplant, or a cornea transplant. She noticed unsteadiness of gait and forgetfulness at the age of 65 years. One month later, unsteadiness and intellectual deterioration progressed and myoclonic jerks appeared. Cerebrospinal fluid analysis was normal except for an increased concentration of neuron-specific enolase (66 ng/ml, normal < 25) and the presence of 14-3-3 protein. EEGs showed periodic spike/slow–wave complexes (spike–wave complexes). Diffusion-weighted MRI showed abnormal high-intensity signals in the head of the caudate nucleus, putamen and insular cortex.

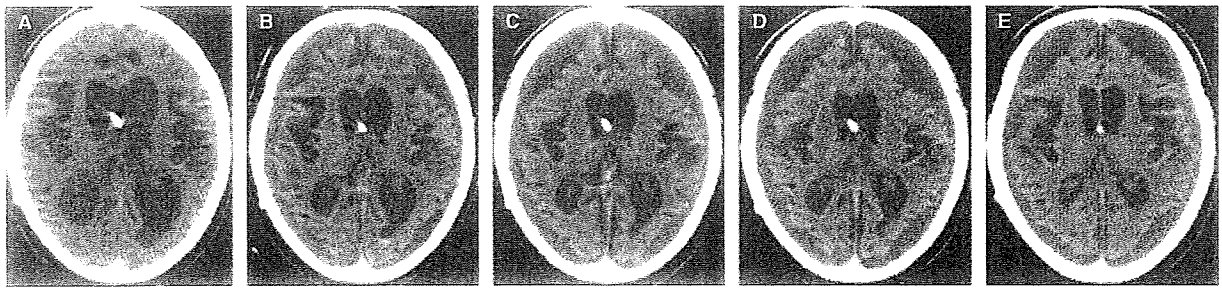

Figure 1. Sequential follow-up CT scans from 12 to 17 months after start of intraventricular PPS infusion. (A) Non-enhanced CT scan 12 months after start of intraventricular PPS infusion. Note the severe cortical and subcortical atrophy with enlargement of ventricular system. (B) Non-enhanced CT scan 13 months after start of intraventricular PPS infusion. Note the subdural fluid collection and the small sedimentation of blood in the left posterior horn. (C, D, E) Non-enhanced CT scan 14, 15, 17 months after start of intraventricular PPS infusion, respectively. The blood sedimentation in the posterior horn disappeared next month and subdural fluid collections were not progressing. No intraventricular hemorrhage was noted in scan E which was taken 7 days before death.

Genetic analysis of the *PrP* gene revealed methionine homozygosity at codon 129 and no mutations. The patient continued to deteriorate and became doubly incontinent, bed-bound and mute. Five months after the onset of symptoms, she developed akinetic mutism. Seven months after onset, the myoclonic jerks and spike–wave complexes disappeared. Ten months after onset, treatment with intraventricular PPS administration commenced under signed informed consent from her family. She received implantation of a right ventricular catheter and an epigastric subcutaneous drug infusion pump (Archimedes; 20-ml reservoir, flow rate 0.5 ml/24 h; Codman & Shurtleff Inc, Raynham, MA, USA). Using a reported protocol (5), infusion of intraventricular PPS (SP 54; bene-Arzneimittel GmbH, Munich, Germany) was started at 1 μg/kg/day, with subsequent escalation to the dose of 60 μg/kg/day 7 months later, and to the target dose of 120 μg/kg/day 15 months later, which continued until she died. However, her clinical condition did not improve and she still displayed akinetic mutism. A series of brain CT examinations demonstrated progressive brain atrophy, a transient intraventricular minor hemorrhage at the time of 13 months later, and a non-progressive collection of subdural fluid until 7 days before death (Fig. 1). Her clinical condition did not deteriorate from the time of 12 to 16 months. Monthly blood cell counts and coagulation measurements were normal. Twenty-seven months after onset, at age 68 years, the patient died of pneumonia which occurred 11 days before death and was aggravated.

Methods

Autopsy was performed within 2 h after death. The right temporal pole of the brain was dissected out and stored at −70°C. The other parts of the brain were fixed in neutral buffered formalin. Sections of representative areas of the brain were stained with hematoxylin–eosin, Klüver–Barrera and immunohistochemical methods.

Immunohistochemical staining

The following primary antibodies were used: anti-phosphorylated α-synuclein (monoclonal; Wako, Osaka, Japan), anti-phosphorylated tau (AT8, monoclonal; Fitzgerald, Concord, MA, USA), anti-amyloid β 1–42 (polyclonal; IBL, Takasaki, Japan) and anti-PrP (3F4, monoclonal; Signet, Dedham, MA, USA).

Prion protein analysis

Protease-resistant PrP was extracted from cerebral tissues of this and other sCJD patients as previously described (7). Samples were subjected to 13.5% SDS-PAGE and transferred to polyvinylidene fluoride membrane. 3F4 antibody was used as the primary antibody. Anti-mouse EnVision (Dako, Glostrup, Denmark) was used as the secondary antibody. Enhanced chemiluminescence detection (Amersham Bioscience, Little Chalfont, UK) was used to visualize Western blots. The signal intensities of the blots were quantified with Quantity One software using an imaging device, Vasa Doc 5000 (Bio-Rad Laboratories, Hercules, CA, USA) (7).

For quantitative comparison of protease-resistant PrP levels, we initially analyzed 10-fold diluted samples derived from 0.5 mg wet-weight brain tissue from the temporal pole to identify suitable dilutions. For controls, we included frontal lobe tissues from three sCJD patients (all homozygous for methionine at codon 129 of the *PrP* gene) not treated with intraventricular PPS infusion: two with a type 1 pattern of protease-resistant PrP signals in Western blot analysis (sCJD MM1) whose brains were uniformly, severely atrophied similarly to the

patient's brain, and one with cortical-type sCJD and a type 2 pattern (sCJD MM2C).

Results

Post-mortem neuropathology

The unfixed brain weighed 660 g and showed walnut-shaped severe atrophy. A massive intraventricular hematoma was present. The shape of blood cells in the hematoma was completely preserved, with no infiltration by reactive cells such as macrophages and glial cells. The PPS infusion catheter had been correctly inserted into the right lateral ventricle, and the source of hemorrhage could not be identified. There was extensive, symmetrical cortical atrophy, but the hippocampi were relatively spared.

Microscopy demonstrated extensive neuronal loss and spongiosis in most areas of the cerebral cortices, with collapsed cytoarchitecture. Axonal loss with secondary myelin loss was present in the central white matter, accompanied by a cellular reaction containing both astrocytes and microglial cells throughout the areas of myelin damage. There was widespread gliosis in the basal ganglia, thalami and cerebellar molecular layer. The cerebellar granular layer showed marked neuronal loss with gliosis and axonal loss, accompanied by secondary myelin loss in the cerebellar white matter. Lewy bodies, amyloid plaques and neurofibrillary tangles were not observed. PrP staining showed a widespread synaptic pattern in the cerebral cortices, basal ganglia and thalami. Synaptic staining was also present in the molecular layer of the cerebellum, with intense coarse deposits in the granular layer. No plaque-like PrP deposits were identified in any brain regions. The findings were consistent with the diagnosis of sCJD. There was no laterality in the extent of the neuronal loss, spongiosis, gliosis or synaptic PrP deposition.

Prion protein analysis

Western blot analysis of protease-resistant PrP showed a type 1 pattern (Fig. 2) identical to those of the two classical sCJD MM1 cases. Protease-resistant PrP levels were 1/3 to 1/8 of those in the sCJD patients with no intraventricular PPS treatment.

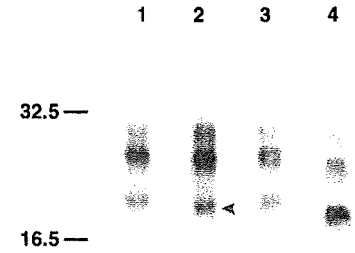

Figure 2. Comparative Western blot analysis of protease-resistant PrP. Protease-resistant PrP is categorized into three types based on the pattern of glycoform and mobility of PrP bands in Western blot analysis. Protease-resistant PrP, type 1, from the brain of this patient (threefold-diluted, lane 2) and three control subjects with sCJD: lane 1, 30-fold-diluted brain sample from an sCJD MM1 subject (65-year-old woman with a survival time of 11 months); lane 3, 20-fold-diluted brain sample from another sCJD MM1 subject (74-year-old woman with a survival time of 16 months); and lane 4, 40-fold-diluted brain sample from an sCJD MM2C subject. An unglycosylated PrP band from this patient (lane 2, arrowhead) mapped slightly lower than those in the other sCJD MM1 subjects (lanes 1 and 3). We normalized signal intensity to the band in lane 2 ($100/mm^2$). After dilution powers were also considered, the corrected signal intensities for lanes 1, 3 and 4 were $680/mm^2$, $300/mm^2$ and $770/mm^2$, respectively.

Discussion

Here, we present a patient with sCJD who was treated with intraventricular PPS for 17 months. The PPS dose of 120 μg/kg/day was well tolerated but was associated with a minor, transient intraventricular hemorrhage and collection of subdural fluid. A fresh intraventricular hematoma found during autopsy probably occurred at the agonal stage, because blood cell shape was preserved and there was no inflammatory cell infiltration. Moreover, this intraventricular hematoma is unlikely to alter the patient's clinical course, because pneumonia which occurred 11 days before death was rapidly aggravated to respiratory failure responsible for her death, and no intraventricular hemorrhage was detected on CT scan 7 days before death.

Pentosan polysulphate is a candidate anti-prion compound that has shown efficacy in animal models (1, 8, 9), and has been administered by intraventricular infusion in several patients (2–6). Thrombocytopenia and abnormal coagulation can occur occasionally with PPS but did not occur in our patient. A minor, transient intraventricular hemorrhage and a non-progressive collection of subdural fluid appeared during PPS treatment but did not influence clinical progression. These findings may have resulted from a pressure imbalance within the intraventricular or subdural spaces caused by PPS infusion, although this speculation requires further proof. Overall, a PPS dose of 120 μg/kg/day seems well-tolerated and does not cause major adverse effects in CJD patients (2–6).

This patient survived for 27 months after the onset of clinical symptoms, which exceeds the mean survival period in national surveillance studies (12.7 months; range, 1–61) in Japan (10). PPS treatment did not alter the clinical course from the initial akinetic mute state. Thus, her prolonged survival might be partially attributable to both good nursing care and active medical interventions for malnutrition and pneumonia. The present study is a preliminary case study in a sCJD patient with pentosan therapy, and placebo-controlled study with PPS infusion will be needed in the future.

Prion protein deposition was not dramatically different between the hemisphere implanted with the catheter and the opposite hemisphere, unlike data reported in a rodent model (1). Here, the treatment started at an advanced clinical stage that may have already involved extensive PrP deposition, whereas treatment in the rodent model started before PrP deposition. In addition, difference of cerebrospinal fluid flow dynamics in the brain ventricular system between rodents and humans might contribute to the discrepancy. However, we found lower levels of abnormal protease-resistant PrP here than in other untreated sCJD patients, suggesting that PPS infusion might suppress the accumulation of abnormal PrP in the brain.

This speculation requires to be further evaluated, because there are possibilities that the gap of abnormal PrP levels between the patient and the control subjects might be attributable to the difference in disease durations or brain sampling regions, or to the regional variety of abnormal PrP deposition. These possibilities could not be evaluated in the present study because of limited sample availability.

Acknowledgements

The intraventricular PPS trial in this case was supported by a grant from the Japanese Ministry of Health, Labor and Welfare (H19-nanji-ippan-006).

References

1. Doh-ura K, Ishikawa K, Murakami-Kubo I et al. Treatment of transmissible spongiform encephalopathy by intraventricular drug infusion of animal models. J Virol 2004;**78**: 4999–5006.
2. Parry A, Baker I, Stacey R, Wimalaratna S. Long term survival in a patient with variant Creutzfeldt–Jakob disease treated with intraventricular pentosan polysulphate. J. Neurol Neurosurg Psychiat 2007;**78**:733–4.
3. Todd NV, Morrow J, Doh-ura K et al. Cerebroventricular infusion of pentosan polysulphate in human variant Creutzfeldt–Jakob disease. J Infect 2005;**50**:394–6.
4. Whittle IR, Knight RSG, Will RG. Unsuccessful intraventricular pentosan polysulphate treatment of variant Creutzfeldt–Jakob disease. Acta Neurochir (Wien) 2006;**148**: 677–9.
5. Rainov NG, Tsuboi Y, Krolak-Salmon P, Vighetto A, Doh-Ura K. Experimental treatments for human transmissible spongiform encephalopathies: is there a role for pentosan polysulfate? Expert Opin Biol Ther 2007;**7**:713–26.
6. Bone I, Belton L, Walker AS, Darbyshire J. Intraventricular pentosan polysulphate in human prion diseases: an observational study in the UK. Eur J Neurol 2008;**15**: 458–64.
7. Hizume M, Kobayashi A, Teruya K et al. Human Prion Protein (PrP) 219K is converted to PrPSc but shows heterozygous inhibition in variant Creutzfeldt–Jakob disease infection. J Biol Chem 2009;**284**:3603–9.
8. Farquhar C, Dickinson A, Bruce M. Prophylactic potential of pentosan polysulphate in transmissible spongiform encephalopathies. Lancet 1999;**353**:117.
9. Ladogana A, Casaccia P, Ingrosso L et al. Sulphate polyanions prolong the incubation period of scrapie-infected hamsters. J Gen Virol 1992;**73**:661–5.
10. Mizusawa H. Prion disease – an overview. Neurol Med 2005;**63**:409–16.

Acta Neurol Scand DOI: 10.1111/j.1600-0404.2009.01255.x

ACTA NEUROLOGICA
SCANDINAVICA

Cerebrospinal fluid metabolite and nigrostriatal dopaminergic function in Parkinson's disease

Ishibashi K, Kanemaru K, Saito Y, Murayama S, Oda K, Ishiwata K, Mizusawa H, Ishii K. Cerebrospinal fluid metabolite and nigrostriatal dopaminergic function in Parkinson's disease.
Acta Neurol Scand: DOI: 10.1111/j.1600-0404.2009.01255.x.

Objectives – To evaluate the association between cerebrospinal fluid (CSF) homovanillic acid (HVA) concentrations and nigrostriatal dopaminergic function assessed by positron emission tomography (PET) imaging with carbon-11-labeled 2β-carbomethoxy-3β-(4-fluorophenyl)-tropane (^{11}C-CFT), which can measure the dopamine transporter (DAT) density, in Parkinson's disease (PD). *Methods* – ^{11}C-CFT PET scans and CSF examinations were performed on 21 patients with PD, and six patients with non-parkinsonian syndromes (NPS) as a control group. *Results* – In the PD group, CSF HVA concentrations were significantly correlated with the striatal uptake of ^{11}C-CFT ($r = 0.76$, $P < 0.01$). However, in the NPS group, two indices were within the normal range. *Conclusions* – In PD, CSF HVA concentrations correlate with nigrostriatal dopaminergic function. Therefore, CSF HVA concentrations may be an additional surrogate marker for estimating the remaining nigrostriatal dopaminergic function in case that DAT imaging is unavailable.

K. Ishibashi[1,2], K. Kanemaru[3], Y. Saito[4], S. Murayama[5], K. Oda[2], K. Ishiwata[2], H. Mizusawa[1], K. Ishii[2]

[1]Department of Neurology and Neurological Science, Graduate School, Tokyo Medical and Dental University, Tokyo, Japan; [2]Positron Medical Center, Tokyo Metropolitan Institute of Gerontology, Tokyo, Japan; [3]Department of Neurology, Tokyo Metropolitan Geriatric Hospital, Tokyo, Japan; [4]Department of Pathology, Tokyo Metropolitan Geriatric Hospital, Tokyo, Japan; [5]Department of Neuropathology, Tokyo Metropolitan Institute of Gerontology, Tokyo, Japan

Key words: cerebrospinal fluid; dopamine transporter; homovanillic acid; Parkinson's disease; positron emission tomography; ^{11}C-CFT

Kenji Ishii, MD, Positron Medical Center, Tokyo Metropolitan Institute of Gerontology, 1-1 Nakacho, Itabashi-ku, Tokyo 173-0022, Japan
Tel.: +81 3 3964 3241
Fax: +81 3 3964 2188
e-mail: ishii@pet.tmig.or.jp

Accepted for publication June 25, 2009

Introduction

In humans, homovanillic acid (HVA) is the major end-product of dopamine metabolism. The HVA in the cerebrospinal fluid (CSF) is largely derived from the nigrostriatal dopaminergic pathway; therefore, HVA concentration in the CSF has been used as an index of dopamine synthesis and presumed to reflect nigrostriatal dopaminergic function. However, even with the availability of a rigorous collection protocol, especially with respect to puncture time and pre-procedural resting, considerable inter-individual and intra-individual variability has been reported with regard to the concentration of CSF HVA in subjects with normal nigrostriatal function (1–3). Therefore, the extent to which CSF HVA concentrations reflect the nigrostriatal dopaminergic function is still unknown, and no study has specifically elucidated the association between the concentration of CSF HVA and the function of nigrostriatal dopamine.

Many studies have shown that the concentration of CSF HVA substantially reduces in patients with Parkinson's disease (PD), which is a neurodegenerative disorder caused by nigrostriatal dopaminergic dysfunction (4–12). However, the extent of reduction also varied a great deal among patients with PD. Because of the variability, the relationship of clinical disability with CSF HVA concentrations and the accuracy of CSF HVA concentrations in differentiating PD from other parkinsonian syndromes have yet to be determined. Several authors have reported an inverse relationship between CSF HVA concentrations and the clinical severity (5–7, 10, 11), while others have denied such a relationship (9, 12, 13). Other neurodegenerative disorders caused by the dysfunction of nigrostriatal dopaminergic system, such as multiple system atrophy (MSA), progressive

supranuclear palsy (PSP) and corticobasal degeneration, also show the reductions of CSF HVA concentrations as compared to normal subjects (8, 14, 15). Therefore, the usefulness of measuring CSF HVA concentrations in daily clinical practice has not yet been established.

In order to address the physiological and pathophysiological backgrounds of these issues, we evaluated the correlation between CSF HVA concentrations and nigrostriatal dopaminergic function. Furthermore, we have discussed the mechanism by which the concentration of CSF HVA reduces in patients with PD.

As means of evaluating nigrostriatal dopaminergic function, we performed carbon-11-labeled 2β-carbomethoxy-3β-(4-fluorophenyl)-tropane (^{11}C-CFT) positron emission tomography (PET) scans which can reveal the dopamine transporter (DAT) density in the striatum. DAT imaging has been recognized as a standard marker for the diagnosis of PD, because it is a very sensitive, reproducible, and reliable marker of nigrostriatal dopaminergic function (16–21).

Materials and methods

Subjects

The present study was a retrospective study. The subjects comprised 35 patients [19 men and 16 women; age 60–83 years (mean age = 71.7 years, SD = 6.0)]. They visited the neurological outpatient clinic at Tokyo Metropolitan Geriatric Hospital from April 2001–November 2004. Of the 35 patients, 29 had parkinsonian symptoms and on the basis of each clinical criteria (22–24), 21 were diagnosed with PD, three with MSA, and five with PSP. The remaining six patients had no parkinsonian symptoms: three were clinically diagnosed with Alzheimer's disease (AD), two with spinocerebellar degeneration (SCD), and one with amyotrophic lateral sclerosis (ALS). Table 1 shows the demographic data. The patients with MSA and PSP were classified in the patients with non-PD (NPD) group, while the patients with AD, SCD and ALS were classified in the patients with non-parkinsonian syndromes (NPS) group. The CSF examinations and the ^{11}C-CFT PET scans were performed within 5 months of each other. None of the patients had any concomitant hereditary disorder that could cause parkinsonian symptoms. All the patients were drug naive.

The normal range of HVA was determined by examining the CSF of 13 normal control subjects [five men and eight women; age, 65–88 years (mean = 77.2 years, SD = 8.2)]. Similarly, the normal range for nigrostriatal dopaminergic function was determined by performing ^{11}C-CFT PET scans of eight normal control subjects [five men and three women; age, 55–74 years (mean age = 62.3 years, SD = 6.9)]. All the control subjects were healthy and did not have any underlying diseases or abnormities, as determined on the basis of their medical history and their physical and neurological examinations. None of them were on any medications at the time of the study. All the subjects also underwent routine MRI examinations.

All the CSF examinations and ^{11}C-CFT PET scans were performed for research. This study protocol was approved by the Ethics Committee of the Tokyo Metropolitan Institute of Gerontology and written informed consents were obtained from all the participants.

CSF analysis

Lumbar puncture was performed in the lateral decubitus position to obtain CSF samples from each subject. The first few milliliter of CFS was discarded. The next 3 ml of CFS was used for routine determinations of cell counts, protein and sugar and an additional 2 ml was stored at −70°C until the assays were preformed. The concentration of CSF HVA was measured by injecting 80 μl CSF

Table 1 Demographics of patients and control subjects

	Subjects				Striatal uptake of ^{11}C-CFT	
	n	M:F	Age (years)	Duration (years)	(Uptake ratio index)	CSF HVA (ng/ml)
Parkinson's disease	21	11:10	72.9 ± 5.0	1.8 ± 1.3	0.94 ± 0.20	12.8 ± 9.35
Hoehn-Yahr 1	1	1:0	62	1	1.38	36.8
Hoehn-Yahr 2	8	4:4	71.6 ± 4.6	1.4 ± 0.9	1.03 ± 0.14	15.6 ± 9.4
Hoehn-Yahr 3	12	6:6	74.7 ± 3.9	2.1 ± 1.5	0.85 ± 0.17	8.9 ± 5.4
Non-Parkinson's disease	8	4:4	70.5 ± 7.7	1.6 ± 0.8	1.00 ± 0.19	16.4 ± 7.7
Non-parkinsonian syndromes	6	4:2	68.8 ± 6.3	4.5 ± 2.4	2.48 ± 0.28	31.9 ± 13.0
Control for PET study	8	5:3	62.3 ± 6.9		2.68 ± 0.44	
Control for CSF study	13	5:8	77.2 ± 8.2			36.0 ± 13.8

Data are expressed as mean ± SD; *n* = number, CSF, cerebrospinal fluid; HVA, homovanillic acid.

samples into a high-performance liquid chromatography system equipped with 16 electrochemical sensors (CEAS Model 5500; ESA, Bedford, MA, USA), as described previously (14).

PET imaging

^{11}C-CFT PET data acquisition – PET studies were performed at the Positron Medical Center, Tokyo Metropolitan Institute of Gerontology using a SET 2400W scanner (Shimadzu, Kyoto, Japan) in the three-dimensional scanning mode (25). The ^{11}C-CFT was prepared as described previously (26). Each subject received an intravenous bolus injection of 388 ± 75 (mean ± SD) MBq of ^{11}C-CFT. Each subject was then placed in the supine position with their eyes closed in the PET camera gantry. The head was immobilized with a customized head holder in order to align the orbitomeatal line parallel to the scanning plane. To measure the uptake of ^{11}C-CFT, a static scan was performed for 75–90 min after the injection. The specific activity at the time of injection ranged from 7.1–119.6 GBq/μmol. The transmission data were acquired using a rotating ^{68}Ga/^{68}Ge rod source for attenuation correction. Images of 50 slices were obtained with a resolution of 2 × 2 × 3.125 mm voxels and a 128 × 128 matrix.

Analysis of ^{11}C-CFT PET images – Image manipulations were carried out by using the Dr View software (version R2.0; AJS, Tokyo, Japan). The individual PET images were resliced in the transaxial direction, parallel to the anterior–posterior intercommissural (AC–PC) line. Circular regions of interest (ROIs) were placed with reference to the brain atlas and individual MRI images. Five ROIs (diameter, 8 mm) were placed on the striatum on both the left and right sides in each of the three contiguous slices (the AC–PC plane, and regions 3.1 and 6.2 mm above the AC–PC line). Of the five ROIs, one ROI was placed on the caudate and four on the putamen. A total of 50 ROIs (diameter, 10 mm) were selected throughout the cerebellar cortex in five contiguous slices. To evaluate the striatal uptake of ^{11}C-CFT, we calculated the uptake ratio index by the following formula (17, 18), as previously validated (27, 28).

$$\text{Uptake ratio index} = (\text{activity in the striatum} - \text{activity in the cerebellum}) / (\text{activity in the cerebellum}).$$

Statistical analysis

Differences in the averages were tested using a Student's *t*-test. Correlations between the two groups were assessed by linear regression analysis with Pearson's correlation test. $P < 0.01$ was considered to indicate statistical significance.

Results

The inter-individual variability in the concentrations of CSF HVA in each group was relatively large (Fig. 1A). CSF HVA concentrations in both the PD ($P < 0.01$) and NPD groups ($P < 0.01$) were significantly lower than that in the control group (mean ± 2SD, 36.0 ± 27.6), while no significant difference was observed between the NPS and control groups.

The striatal uptake of ^{11}C-CFT in the PD and NPD groups was below the normal range (mean ± 2SD, 2.68 ± 0.87; Fig. 1B). In the PD group, CSF HVA concentrations were significantly

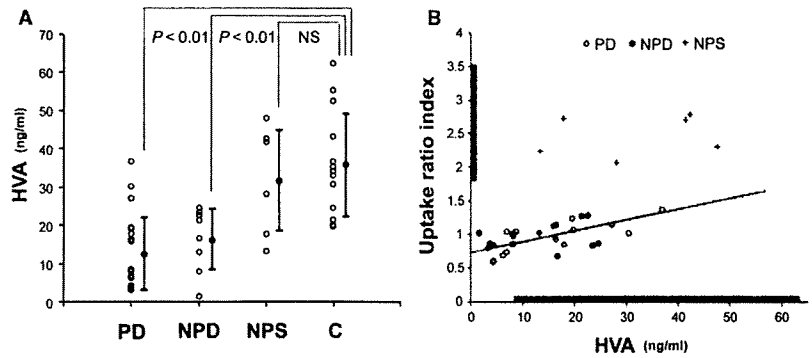

Figure 1. (A) The comparison of CSF HVA concentrations among the disease and control groups. Vertical bars represent mean ± SD. (B) Relationship between CSF HVA concentrations and the striatal uptake of ^{11}C-CFT. A solid line represents the regression line for the PD group. Linear correlation was significant ($r = 0.76$; $P < 0.01$). The grey bars beside the *x*- and *y*-axes represent the normal range (mean ± 2SD) for HVA (36.0 ± 27.6) and the striatal uptake of ^{11}C-CFT (2.68 ± 0.87). PD, Parkinson's disease; NPD, non-Parkinson's disease with parkinsonism; NPS, non-parkinsonian syndromes; C, controls; NS, not significant; CSF, cerebrospinal fluid; HVA, homovanillic acid.

correlated with the striatal uptake of ^{11}C-CFT ($r = 0.76$, $P < 0.01$). In the NPD group, although the correlation between the two indices was not statistically significant, the distribution pattern between the two indexes showed the same tendency as that in the PD group. However, in the NPS group, both CSF HVA concentrations and the striatal uptake of ^{11}C-CFT were within the normal ranges.

Discussion

We evaluated the correlation between CSF HVA concentrations and nigrostriatal dopaminergic function by performing ^{11}C-CFT PET scans. ^{11}C-CFT PET scans showed that all patients with PD and NPD had the dysfunction of nigrostriatal dopaminergic system and all patients with NPS had normal function. The CSF HVA concentrations of all patients with PD and NPD were significantly lower than those of normal subjects, in accordance with previous studies (5–12, 14, 15), whereas, there was no significant difference in CSF HVA concentrations between normal subjects and patients with NPS. These results suggest that CSF HVA concentrations could reflect nigrostriatal dopaminergic function. However, in accordance with previous reports (1–9, 13, 14), all groups showed large inter-individual variability in CSF HVA concentrations and relatively wide overlaps among groups were found. Therefore, in clinical practice, measuring CSF HVA concentrations may be of limited value in the diagnosis of PD.

This is the first study that investigated the correlation between CSF HVA concentrations and nigrostriatal dopaminergic dysfunction. Regardless of relatively high inter-individual variability, CSF HVA concentrations in the PD group showed a considerably high correlation with the striatal uptake of ^{11}C-CFT. The NPD group with nigrostriatal dopaminergic dysfunction showed the same tendency as the PD group, although without significant correlation probably because of the small number of patients. On the other hand, the NPD group with normal nigrostriatal dopaminergic function showed normal ranges in both the HVA level and the striatal uptake of ^{11}C-CFT. Therefore, CSF HVA concentrations may be an additional surrogate maker for estimating the nigrostriatal dopaminergic function in patients with PD, in case that DAT imaging, which has been recognized as a standard maker for the diagnosis of PD, is unavailable.

It is important to note that the DAT images of patients with PD are unique; in the pre-symptomatic phase the reduction in the availability of striatal DAT was detected, presumably as a result of both the degeneration of nigral dopaminergic cells and the compensatory downregulation of DATs on the presynaptic site to maintain normal synaptic dopamine concentrations (17–21). Furthermore, the striatal DAT availability declined at an annual rate of 5–10% (19, 21, 29–31).

Considering our results and the unique characteristics of the DAT images, a possible explanation about the association between CSF HVA concentrations and the striatal uptake of ^{11}C-CFT is as follows (Fig. 2). The first stage of the disease is a compensatory and asymptomatic phase. Along with the progression of nigrostriatal degeneration, the striatal DAT availability begins to decrease, as described earlier (17–21). However, due to several compensatory mechanisms, including the downregulation of DATs and the upregulation of dopamine synthesis, the striatal dopamine concentrations are kept within the normal range (32). As a result, CSF HVA concentrations are also kept in the normal range because CSF HVA is the major end-product of striatal dopamine metabolism. This phase would show relatively large intra-individual and inter-individual variability in CSF HVA concentrations, as observed in subjects with normal nigrostriatal dopaminergic function, because of the reserve capacity for adjusting its levels. The second stage of the progression of the disease is an advanced and symptomatic phase. The compensatory mechanisms to maintain normal synaptic

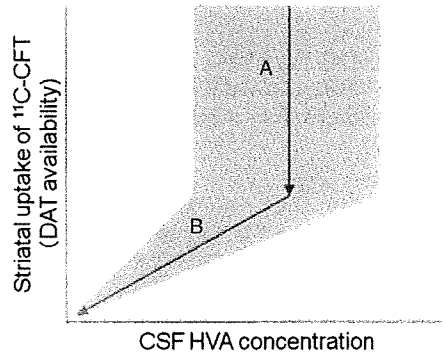

Figure 2. Schematic representation of the mechanism of CSF HVA reduction in patients with PD. (A) The nigrostriatal degeneration begins with a decrease in DAT availability, but due to several compensatory mechanisms, striatal dopamine concentrations (CSF HVA concentrations) are maintained within the normal range. There is a large variability with regard to CSF HVA concentrations. (B) The compensatory mechanisms break down and striatal dopamine concentrations (CSF HVA concentrations) begin to decrease along with the decrease in DAT availability. The variability in CSF HVA concentrations gradually becomes smaller. The grey zone represents the range of variability in CSF HVA concentrations to the striatal uptake of ^{11}C-CFT. DAT, dopamine transporter; CSF, cerebrospinal fluid, HVA, homovanillic acid.

dopamine concentrations break down and the striatal dopamine and CSF HVA concentrations begin to decrease with the reduction of DAT availability. In this phase, the intra-individual and inter-individual variability in CSF HVA concentrations would gradually decrease because of a lesser capacity for adjusting its levels. Consequently, CSF HVA concentrations remain within a narrow range that corresponds to the remaining nigrostriatal dopaminergic function. In symptomatic patients with PD, CSF HVA concentrations correlate with nigrostriatal dopaminergic function. To verify this explanation, a study with larger number of patients is needed.

In conclusion, we found a significant correlation between CSF HVA concentrations and the striatal uptake of ^{11}C-CFT in patients with PD. Although we should remember that CSF HVA concentrations show large variability, CSF HVA concentrations may be an additional surrogate maker for estimating the remaining nigrostriatal dopaminergic function in patients with PD in case that DAT imaging is unavailable.

Acknowledgements

The authors thank Mr Keiichi Kawasaki and Ms Hiroko Tsukinari for their technical assistance. This study was supported by Grants-in-Aid for Neurological and Psychiatric Research (S. Murayama, Y. Saito and K. Ishii) and Research for Longevity (S. Murayama, Y. Saito and K. Ishii) from the Ministry of Health, Labor and Welfare of Japan; for Scientific Research (B) No. 20390334 (K. Ishiwata) from the Japan Society for the Promotion of Science; for the Program for Promotion of Fundamental Studies in Health Sciences of the National Institute of Biomedical Innovation, Japan (No: 06–46, K. Ishiwata); and for Long-Term Comprehensive Research on Age-associated Dementia from the Tokyo Metropolitan Institute of Gerontology (K. Kanemaru, S. Murayama and K. Ishii).

References

1. Seeldrayers P, Messina D, Desmedt D, Dalesio O, Hildebrand J. CSF levels of neurotransmitters in Alzheimer-type dementia. Effects of ergoloid mesylate. Acta Neurol Scand 1985;**71**:411–4.
2. Ballenger JC, Post RM, Goodwin FK. Neurochemistry of cerebrospinal fluid in normal individuals. In: Wood JH, ed. Neurobiology of cerebrospinal fluid. New York: Plenum Press, 1982;**2**:143–55.
3. Hildebrand J, Bourgeois F, Buyse M, Przedborski S, Goldman S. Reproducibility of monoamine metabolite measurements in human cerebrospinal fluid. Acta Neurol Scand 1990;**81**:427–30.
4. Parkinson Study Group. Cerebrospinal fluid homovanillic acid in the DATATOP study on Parkinson's disease. Parkinson Study Group. Arch Neurol 1995;**52**:237–45.
5. Chia LG, Cheng FC, Kuo JS. Monoamines and their metabolites in plasma and lumbar cerebrospinal fluid of Chinese patients with Parkinson's disease. J Neurol Sci 1993;**116**:125–34.
6. Chase TN, Ng LK. Central monoamine metabolism in Parkinson's disease. Arch Neurol 1972;**27**:486–91.
7. Korf J, van Praag HM, Schut D, Nienhuis RJ, Lakke JP. Parkinson's disease and amine metabolites in cerebrospinal fluid: implications for L-Dopa therapy. Eur Neurol 1974; **12**:340–50.
8. Abdo WF, De Jong D, Hendriks JC et al. Cerebrospinal fluid analysis differentiates multiple system atrophy from Parkinson's disease. Mov Disord 2003;**19**:571–9.
9. Davidson DL, Yates CM, Mawdsley C, Pullar IA, Wilson H. CSF studies on the relationship between dopamine and 5-hydroxytryptamine in Parkinsonism and other movement disorders. J Neurol Neurosurg Psychiatry 1977;**40**: 1136–41.
10. Tohgi H, Abe T, Takahashi S, Ueno M, Nozaki Y. Cerebrospinal fluid dopamine, norepinephrine, and epinephrine concentrations in Parkinson's disease correlated with clinical symptoms. Adv Neurol 1990;**53**:277–82.
11. Mayeux R, Stern Y. Intellectual dysfunction and dementia in Parkinson disease. Adv Neurol 1983;**38**:211–27.
12. Gibson CJ, Logue M, Growdon JH. CSF monoamine metabolite levels in Alzheimer's and Parkinson's disease. Arch Neurol 1985;**42**:489–92.
13. Kurlan R, Goldblatt D, Zaczek R et al. Cerebrospinal fluid homovanillic acid and parkinsonism in Huntington's disease. Ann Neurol 1988;**24**:282–4.
14. Kanemaru K, Mitani K, Yamanouchi H. Cerebrospinal fluid homovanillic acid levels are not reduced in early corticobasal degeneration. Neurosci Lett 1998;**245**:121–2.
15. Ruberg M, Javoy-Agid F, Hirsch E et al. Dopaminergic and cholinergic lesions in progressive supranuclear palsy. Ann Neurol 1985;**18**:523–9.
16. Nurmi E, Bergman J, Eskola O et al. Reproducibility and effect of levodopa on dopamine transporter function measurements: a [18F]CFT PET study. J Cereb Blood Flow Metab 2000;**20**:1604–9.
17. Frost JJ, Rosier AJ, Reich SG et al. Positron emission tomographic imaging of the dopamine transporter with 11C-WIN 35,428 reveals marked declines in mild Parkinson's disease. Ann Neurol 1993;**34**:423–31.
18. Wong DF, Yung B, Dannals RF et al. In vivo imaging of baboon and human dopamine transporters by positron emission tomography using [11C]WIN 35,428. Synapse 1993;**15**:130–42.
19. Nurmi E, Bergman J, Eskola O et al. Progression of dopaminergic hypofunction in striatal subregions in Parkinson's disease using [18F]CFT PET. Synapse 2003; **48**:109–15.
20. Rinne JO, Ruottinen H, Bergman J, Haaparanta M, Sonninen P, Solin O. Usefulness of a dopamine transporter PET ligand [(18)F]beta-CFT in assessing disability in Parkinson's disease. J Neurol Neurosurg Psychiatry 1999;**67**:737–41.
21. Nurmi E, Ruottinen HM, Kaasinen V et al. Progression in Parkinson's disease: a positron emission tomography study with a dopamine transporter ligand [18F]CFT. Ann Neurol 2000;**47**:804–8.
22. Hughes AJ, Daniel SE, Kilford L, Lees AJ. Accuracy of clinical diagnosis of idiopathic Parkinson's disease: a clinico-pathological study of 100 cases. J Neurol Neurosurg Psychiatry 1992;**55**:181–4.
23. Litvan I, Agid Y, Calne D et al. Clinical research criteria for the diagnosis of progressive supranuclear palsy (Steele-Richardson-Olszewski syndrome): report of the NINDS-SPSP international workshop. Neurology 1996; **47**:1–9.

24. Gilman S, Low PA, Quinn N et al. Consensus statement on the diagnosis of multiple system atrophy. J Auton Nerv Syst 1998;**74**:189–92.
25. Fujiwara T, Watanuki S, Yamamoto S et al. Performance evaluation of a large axial field-of-view PET scanner: SET-2400W. Ann Nucl Med 1997;**11**:307–13.
26. Kawamura K, Oda K, Ishiwata K. Age-related changes of the [11C]CFT binding to the striatal dopamine transporters in the Fischer 344 rats: a PET study. Ann Nucl Med 2003;**17**:249–53.
27. Hashimoto M, Kawasaki K, Suzuki M et al. Presynaptic and postsynaptic nigrostriatal dopaminergic functions in multiple system atrophy. Neuroreport 2008;**19**:145–50.
28. Ishibashi K, Ishii K, Oda K, Kawasaki K, Mizusawa H, Ishiwata K. Regional analysis of age-related decline in dopamine transporters and dopamine D(2)-like receptors in human striatum. Synapse 2008;**63**:282–90.
29. Staffen W, Mair A, Unterrainer J, Trinka E, Ladurner G. Measuring the progression of idiopathic Parkinson's disease with [123I] beta-CIT SPECT. J Neural Transm 2000; **107**:543–52.
30. Chouker M, Tatsch K, Linke R, Pogarell O, Hahn K, Schwarz J. Striatal dopamine transporter binding in early to moderately advanced Parkinson's disease: monitoring of disease progression over 2 years. Nucl Med Commun 2001;**22**:721–5.
31. Marek K, Innis R, van Dyck C et al. [123I]beta-CIT SPECT imaging assessment of the rate of Parkinson's disease progression. Neurology 2001;**57**:2089–94.
32. Lee CS, Samii A, Sossi V et al. In vivo positron emission tomographic evidence for compensatory changes in presynaptic dopaminergic nerve terminals in Parkinson's disease. Ann Neurol 2000;**47**:493–503.

Acta Neuropathol (2009) 117:169–174
DOI 10.1007/s00401-008-0450-7

ORIGINAL PAPER

Olfactory bulb α-synucleinopathy has high specificity and sensitivity for Lewy body disorders

Thomas G. Beach · Charles L. White III · Christa L. Hladik · Marwan N. Sabbagh · Donald J. Connor · Holly A. Shill · Lucia I. Sue · Jeanne Sasse · Jyothi Bachalakuri · Jonette Henry-Watson · Haru Akiyama · Charles H. Adler · The Arizona Parkinson's Disease Consortium

Received: 30 September 2008 / Revised: 20 October 2008 / Accepted: 21 October 2008 / Published online: 4 November 2008

Abstract Involvement of the olfactory bulb by Lewy-type α-synucleinopathy (LTS) is known to occur at an early stage of Parkinson's disease (PD) and Lewy body disorders and is therefore of potential usefulness diagnostically. An accurate estimate of the specificity and sensitivity of this change has not previously been available. We performed immunohistochemical α-synuclein staining of the olfactory bulb in 328 deceased individuals. All cases had received an initial neuropathological examination that included α-synuclein immunohistochemical staining on sections from brainstem, limbic and neocortical regions, but excluded olfactory bulb. These cases had been classified based on their clinical characteristics and brain regional distribution and density of LTS, as PD, dementia with Lewy bodies (DLB), Alzheimer's disease with LTS (ADLS), Alzheimer's disease without LTS (ADNLS), incidental Lewy body disease (ILBD) and elderly control subjects. The numbers of cases found to be positive and negative, respectively, for olfactory bulb LTS were: PD 55/3; DLB 34/1; ADLS 37/5; ADNLS 19/84; ILBD 14/7; elderly control subjects 5/64. The sensitivities and specificities were, respectively: 95 and 91% for PD versus elderly control; 97 and 91% for DLB versus elderly control; 88 and 91% for ADLS versus elderly control; 88 and 81% for ADLS versus ADNLS; 67 and 91% for ILBD versus elderly control. Olfactory bulb synucleinopathy density scores correlated significantly with synucleinopathy scores in all other brain regions (Spearman *R* values between 0.46 and 0.78) as well as with scores on the Mini-Mental State Examination and Part 3 of the Unified Parkinson's Disease Rating Scale (Spearman *R* −0.27, 0.35, respectively). It is concluded that olfactory bulb LTS accurately predicts the presence of LTS in other brain regions. It is suggested that olfactory bulb biopsy be considered to confirm the diagnosis in PD subjects being assessed for surgical therapy.

Keywords Parkinson's disease, surgery · Deep brain stimulation · Gene therapy · Transplantation · Dementia with Lewy bodies, diagnosis, therapy, clinical trial · α-Synuclein, Lewy bodies, incidental Lewy body disease · Biopsy · Olfactory bulb

T. G. Beach (✉) · M. N. Sabbagh · D. J. Connor · H. A. Shill · L. I. Sue · J. Sasse · J. Bachalakuri · J. Henry-Watson
Sun Health Research Institute, 10515 West Santa Fe Drive, Sun City, AZ 85351, USA
e-mail: thomas.beach@bannerhealth.org; thomas.beach@sunhealth.org

C. L. White III · C. L. Hladik
University of Texas Southwestern Medical Center, Dallas, TX, USA

H. Akiyama
Tokyo Institute of Psychiatry, Tokyo, Japan

C. H. Adler
Mayo Clinic, Scottsdale, AZ, USA

Introduction

It has long been observed that subjects with Parkinson's disease (PD) have decreased olfactory sensation [1, 10, 17, 24]. Attempts to use tests of olfaction for clinical diagnosis have had mixed results, however, due to loss of olfactory ability in other conditions as well [22, 32]. Lewy bodies and synucleinopathy have been reported to be present in the olfactory bulbs of subjects with PD and dementia with Lewy bodies (DLB) as well as asymptomatic subjects with incidental Lewy body disease (ILBD) [5, 7, 9, 19, 35], suggesting that olfactory bulb synucleinopathy is present in several Lewy body disorders and occurs at an early stage of

disease. Additionally, synucleinopathy and tauopathy have been reported to co-exist in affected olfactory bulb neurons of subjects with Alzheimer's disease [11].

The presence of synucleinopathy in the olfactory bulb makes it theoretically possible to improve upon clinical diagnostic accuracy for Lewy body disorders during life, using olfactory bulb biopsy. However, the specificity and sensitivity of ollfactory bulb synucleinopathy should be established in a large autopsy series. To achieve this, we undertook immunohistochemical α-synuclein staining of the olfactory bulb in 328 autopsied elderly individuals.

Materials and methods

Human subjects

The study took place at Sun Health Research Institute (SHRI), which is a non-profit organization located in the Sun Cities retirement communities of northwest metropolitan Phoenix, AZ. Sun Health Research Institute and the Mayo Clinic Arizona are the principal members of the Arizona Parkinson's Disease Consortium. Brain necropsies and neuropathological examinations were performed on elderly subjects who had volunteered for the SHRI Brain Donation Program [3]. The Brain Donation Program has been approved by the Institutional Review Board of Sun Health Research Institute. Subjects were chosen by searching the Brain Donation Program Database for all those that died between 1 January 1997 and 31 December 2006 with clinicopathologic diagnoses of control (no clinical history of dementia or parkinsonism), PD, DLB and AD, for whom olfactory bulb tissue was available and for whom a complete set of brain blocks had been stained immunohistochemically for α-synuclein. The brain regions were chosen based on published staging procedures for Parkinson's disease [6] and dementia with Lewy bodies [30] and therefore included anterior medulla, anterior pons, midbrain, amygdala, cingulate gyrus, middle temporal gyrus, middle frontal gyrus and inferior parietal lobule.

Subjects received standardized neuropathological examinations as described previously [3]. Specific consensus diagnostic criteria were used for Alzheimer's disease (AD) [40], Parkinson's disease [13] and dementia with Lewy bodies [31]. For both AD and DLB, cases received the diagnosis if they were classified as "intermediate" or "high" probabilities in their respective classification schemes. Cases with Lewy-type synucleinopathy but not meeting these diagnostic criteria were designated as either incidental Lewy body disease (ILBD) or Alzheimer's disease with Lewy-type synucleinopathy (ADLS).

All subjects were clinically characterized by review of medical records, self-report and interviews with spouses and/or caregivers. As part of the Brain Donation Program's standard protocol, 2 years of private medical records are obtained from the subjects' private physicians, both at the time of enrollment and at the time of death. A subset of subjects received standardized neuropsychological and movement disorder assessments at SHRI, including the Mini Mental State Examination (MMSE) and Unified Parkinson's Disease Rating Scale (UPDRS).

Tissue processing and analysis

Paraffin-embedded blocks of anterior medulla, anterior pons, amygdala, cingulate gyrus, middle frontal gyrus, middle temporal gyrus and inferior parietal lobule were initially stained after brain necropsy using an immunoperoxidase method for α-synuclein. Sections were stained after pretreatment with proteinase K [18] using an antiserum raised against an α-synuclein peptide fragment that was phosphorylated at serine 129 [12]. Color development was achieved with an avidin–biotin–horseradish peroxidase complex (ABC) and 3,3′-diaminobenzidine enhanced with nickel ammonium sulfate; the method has been generally described in a prior publication [4]. The same method was later used to stain paraffin-embedded olfactory bulb sections from the 328 cases, for the present study. Lewy bodies and associated neurites in the substantia nigra were identified in 40 μm sections of midbrain stained with thioflavine S. Lewy bodies and associated neurite density were graded in all brain regions as mild, moderate, severe and very severe, according to the templates published by the Dementia with Lewy Bodies Consortium [30].

Statistical analysis

Statistical analyses consisted of Spearman correlation of olfactory bulb synucleinopathy scores with synucleinopathy scores in other brain regions as well as with MMSE and motor UPDRS scores. Logistic regression analysis was used to obtain odds ratios as well as sensitivities and specificities. For the latter determinations, the dependent binary variable in all cases was diagnosis while the sole independent variable was defined by positive or negative evidence of synucleinopathy in the olfactory bulb.

Results

Description of diagnostic groups

Of the 328 subjects with a full set of paraffin blocks available, there were 69 elderly controls, 21 ILBD, 58 PD, 35 DLB, 42 ADLS and 103 AD without synucleinopathy (ADNLS), based on prior evaluations not including

Table 1 Age and neuropathologic diagnoses of study subjects

Diagnosis	*N*	Mean age (SD)	Range
Elderly control (EC)	69	86.0 (5.64)	73–100
Incidental Lewy body disease (ILBD)	21	85.7 (6.33)	73–103
Parkinson's disease (PD)	58	79.7 (6.26)	64–90
Dementia with Lewy bodies[a] (DLB)	35	81.4 (7.34)	64–95
Alzheimer's disease with Lewy synucleinopathy (ADLS)	42	83.5 (7.76)	66–102
Alzheimer's disease without Lewy synucleinopathy (ADNLS)	103	83.5 (8.73)	48–98

Values shown are mean values, with standard deviations in parentheses

[a] All but four cases also met diagnostic criteria for AD

examination of the olfactory bulb (Table 1). The subjects ranged in age from 64 to 103, with mean ages for the diagnostic groups ranging from 79.7 (PD) to 85.7 (ILBD). Of the DLB cases, all but four also fulfilled diagnostic criteria for AD. The cases with combined DLB/AD were classified, for the purposes of this study, only as DLB and were not included in the AD groups.

Morphologic characteristics of olfactory bulb synucleinopathy

In cases showing positive immunostaining for α-synuclein, the stained elements usually resembled neuronal perikaryal cytoplasmic inclusions or neuritic fibers, while a smaller fraction were dot-like, possibly representing presynaptic terminals or fibers cut in cross-section (Fig. 1a–f). In the great majority of cases, both perikaryal cytoplasmic inclusions and fibers were present. Rarely, bulbs contained only perikaryal cytoplasmic inclusions or only neurites. Perikaryal inclusions were mostly in the form of round or irregular areas of cytoplasmic staining. Inclusions resembling classical Lewy bodies, with a distinguishable core-and-halo appearance, were only seen in approximately 10% of cases (Fig. 1d). The neurites were mostly fine and unbranching, with occasional enlarged distorted forms (Fig. 1e) that were similar to Lewy-related neurites reported for other brain regions. The bulb region most frequently and heavily involved was the anterior olfactory nucleus, consisting of multipolar medium-sized neurons (Fig. 1a–d), arranged in small discontinuous groups along the central axis of the bulb. The inner plexiform layer (Fig. 1f) was the next most frequently and heavily affected area and the staining in this layer was always neuritic, without perikaryal inclusions. It is noted here that our usage of the term "anterior olfactory nucleus" is restricted to those neuronal groups that reside within the bulb itself. We did not examine the nucleus of the same name that is located near the ventral brain surface at the junction of the olfactory tract with the anterior perforated substance.

Sensitivity and specificity of olfactory bulb synucleinopathy for Lewy body disorders

The presence of synucleinopathy in the olfactory bulb was highly predictive of synucleinopathy elsewhere in the brain, regardless of the diagnostic classification of cases. The numbers of cases, by diagnosis, found to be positive and negative, respectively, for olfactory bulb Lewy-type

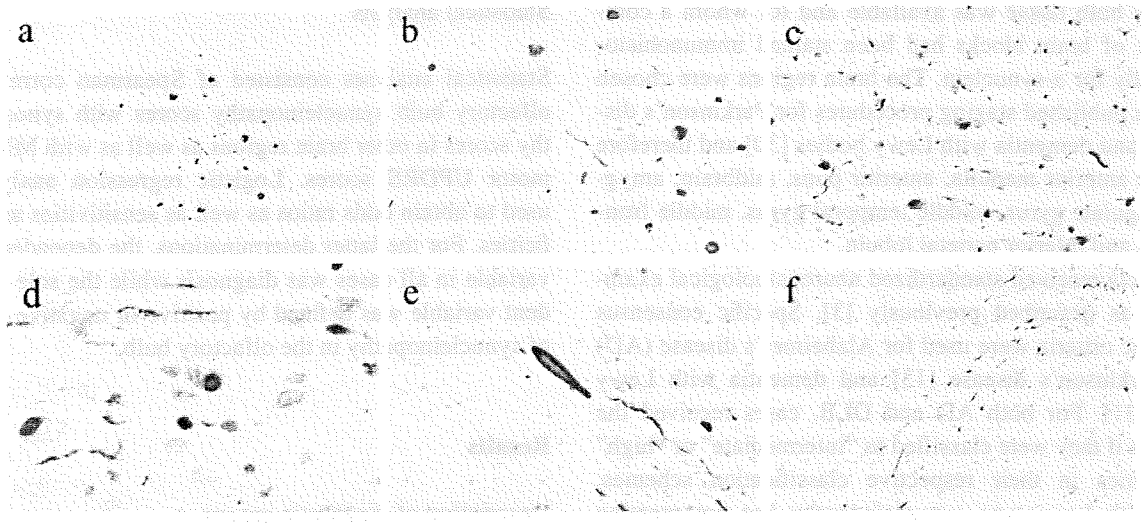

Fig. 1 Olfactory bulb sections depicting α-synuclein-immunoreactive features. **a** Low-magnification photomicrograph of the anterior olfactory nucleus within the olfactory bulb; both neuronal perikaryal cytoplasmic inclusions and neurites are stained. **b** Higher-magnification image of anterior olfactory nucleus from previous *panel*. **c** Anterior olfactory nucleus from another subject, again illustrating both neuronal perikaryal cytoplasmic inclusions and neurites. **d** Lewy body-like inclusion (*center*) within a neuron of the anterior olfactory nucleus. **e** Swollen, dystrophic neurite within the olfactory tract, immunoreactive for α-synuclein, **f** Fibers immunoreactive for α-synuclein, coursing within the internal plexiform layer

Table 2 Odds ratios, 95% confidence intervals, sensitivity and specificity for olfactory bulb synucleinopathy by diagnostic category

Comparison	OR (95% CI)	Sensitivity (%)	Specificity (%)	Wald *P*
PD versus EC	572 (65–5,065)	98	91	<0.000001
DLB versus EC	378 (42–3,373)	97	91	<0.000001
ADLS versus EC	83 (22–305)	89	91	<0.000001
ADLS versus ADNLS	44 (15–126)	89	85	<0.000001
ILBD versus EC	22 (6–78)	69	91	<0.000001

See Table 1 for abbreviations

synucleinopathy were PD 55/3, DLB 34/1, ADLS 37/5, ADNLS 19/84; elderly control subjects without diagnoses of parkinsonism, dementia or ILBD 5/64, ILBD 14/7. Olfactory bulb staining revealed 24 cases (19 among Alzheimer's disease cases, 5 among the elderly control group) that were previously unsuspected to be Lewy body disorders, as brain sections from other regions in these cases had all been negative for α-synuclein. The sensitivities and specificities for specific diagnostic categories (Table 2) were 95% sensitive, 93% specific for the diagnosis of PD versus elderly control; 97% sensitive, 93% specific for DLB versus elderly control; 88% sensitive, 93% specific for ADLS versus control; 88% sensitive, 81% specific for ADLS versus ADNLS; 71% sensitive, 93% specific for ILBD versus control. The results were all statistically significant (Wald $P < 0.00001$).

Correlation of olfactory bulb synucleinopathy score with those in other brain regions

Correlation analysis (Table 3) showed that olfactory bulb synucleinopathy density scores correlated significantly with those in other brain regions, with Spearman correlation coefficients ranging from 0.46 (inferior parietal lobule) to 0.78 (amygdala). All correlations were statistically significant (Spearman $P < 0.0001$).

Correlation of olfactory bulb synucleinopathy score with MMSE and UPDRS scores

Correlation analysis (Table 3) showed that olfactory bulb synucleinopathy density scores correlated significantly with MMSE and UPDRS (motor part) scores, with Spearman correlation coefficients of −0.27 and 0.35, respectively. Both correlations were statistically significant (Spearman $P < 0.0001$).

Discussion

Olfactory bulb synucleinopathy accurately predicts the presence of Lewy body disorders

The results of this investigation show that the presence of synucleinopathy in the olfactory bulb predicts, with greater than 90% sensitivity and specificity, the existence of neuropathologically confirmed PD and DLB. Additionally, olfactory bulb synucleinopathy predicts with high accuracy the presence of Lewy body pathology in subjects with AD. It is probable that olfactory bulb synucleinopathy occurs at early stages of Lewy body disorders as it is present in the majority of cases of ILBD, the suspected preclinical form of PD and/or DLB [2]. These results also show that the severity of olfactory bulb synucleinopathy may serve as a rough guage of the severity of Lewy-related pathology throughout the CNS, as it correlates with the severity of synucleinopathy in the brainstem, limbic regions and neocortex, as well as with measures of the severity of cognitive and motor dysfunction. While it has previously been reported that the olfactory bulb is involved at early stages of Lewy body disorders [7, 19], the sensitivity and specificity of olfactory bulb synucleinopathy for such conditions had not been estimated.

Olfactory bulb biopsy: possible indication for patient selection for PD surgical therapy

Until now, there has not been a practical and ethical option for a biopsy diagnosis of PD. Cortical biopsy has been

Table 3 Spearman correlation of olfactory bulb synucleinopathy density scores with scores in other brain regions and with scores from those subjects that received mini mental state examinations (MMSE, $N = 270$) and unified Parkinson's disease rating scale, Part 3 (UPDRS Motor part, $N = 170$)

IX/X	LC	SN	Amyg	Cing	MTG	MFG	PAR	MMSE	UPDRS
0.69	0.63	0.64	0.78	0.63	0.56	0.61	0.46	−0.27	0.35

All brain region correlations were statistically significant as were the correlations with MMSE and UPDRS (Spearman $P < 0.0001$ for all correlations)

IX/X anterior medulla, including nuclei associated with cranial nerves IX and X; *LC* anterior pons, including locus ceruleus; *SN* midbrain, including substantia nigra; *Amyg* amygdala; *Cing* cingulate gyrus; *MTG* middle temporal gyrus; *MFG* middle frontal gyrus; *PAR* inferior parietal lobule